

SUPPLEMENTAL MATERIAL

Data S1.

Supplemental Methods

On request to the Corresponding author, the data, analytic methods, and study materials will be/have been made available to other researchers for purposes of reproducing the results or replicating the procedure.

Development and maintenance of the Hypertrophic Heart Rat (HHR) and control Normal Heart Rat (NHR) strains

A novel normotensive, hypertrophic rat strain has been generated through selection and cross breeding of Fischer 344 and Spontaneously Hypertensive Rat (SHR) strain progenitors.¹ We had demonstrated previously that the SHR possessed genetic determinants of cardiac hypertrophy, independent of blood pressure.² For the first 4 generations males and females were selected for the HHR line which exhibited elevated left ventricular echo dimensions relative to the corresponding mating pairs in the NHR line. Both lines were stabilized through 21 generations of in-breeding to achieve strain status.³ The control Normal Heart Rat (NHR) was co-derived from the same original F2 population. Thus, the Hypertrophic Heart Rat (HHR) and Normal Heart Rat (NHR) strains constitute genetically stabilized models for investigation of non-load induced hypertrophy, with natural disease history. HHR and NHR genomic analysis has identified variants unique to each strain, including single nucleotide polymorphisms, insertions & deletions, and copy number variations.³ Experiments were performed using male HHR and NHR at ages indicated. This study was confined to single sex evaluation and pooling of sex data avoided as previous studies have identified sex differences which will be further explored in additional studies. All animals were housed under a 12-hour light/dark cycle with water and standard chow provided *ad libitum*.

Echocardiography

Cardiac structure and function were evaluated by transthoracic 2-dimensional B- and M-mode echocardiography (GE Vivid 9; 15mHz i13L linear array transducer) performed under light anesthesia (inhalation of isoflurane at 1.5%) ensuring temperature maintenance of animals. Acquisition and offline analysis was performed with GE EchoPac software. The parasternal short axis was utilized for *systolic parameters* (interventricular septum IVS, left ventricular posterior wall LVPW, left ventricular dimension LVID, fractional shortening FS, ejection fraction EF, heart rate HR), and mitral valve blood flow and tissue Doppler were measured in apical four chamber view for *diastolic parameters* (E/A, isovolumic relaxation time IVRT, mitral valve deceleration time MVDecT, E'/A', E'/E). Normalized parameters for wall dimension indices were calculated for HHR by scaling measured values by the ratio of animal body weight relative to NHR mean. For each measurement at least three consecutive cycles were sampled.

Electrocardiograms

Electrocardiograms (ECG) were obtained under light anesthesia (inhalation of isoflurane at 1.5%) using external clip leads in standard configuration. The ECG signal was amplified (ADInstruments Animal Bio Amp), digitally acquired, filtered, displayed and analyzed using a MacLab data acquisition system.

Hemodynamic measurements

24-h blood pressure profiles in freely moving conscious rats were monitored over a continuous period of 7 days by telemetry. Two weeks prior to recording, rats were implanted with blood pressure telemeters (model TA11PA-C40, Data Sciences International) in the abdominal aorta according to the method detailed by the supplier. Systolic and diastolic blood pressure, and mean arterial pressure were recorded as the reduced mean of a 10-s sampling interval every 10 min using data acquisition and analysis software (Data Sciences International, USA). As previously described⁴, to obtain hemodynamic measures by cardiac catheterization animals were anaesthetized with sodium pentobarbital (60mg/kg) and were intubated and ventilated using positive pressure with a tidal volume of 8 to 10% body weight at 70 breaths/min using room air. A 2F miniaturized combined conductance catheter-micromanometer (Model

SPR-838 Millar instruments, Houston, TX) was inserted into the right carotid artery to obtain aortic blood pressure, and then advanced into the left ventricle until stable pressure-volume (PV) loops were obtained. Data were acquired under steady state conditions and during preload reduction. Using the pressure conductance data a range of functional parameters was then calculated (Lab Chart analysis software). These included end diastolic pressure (EDP), maximum rate of pressure change in the ventricle (+dP/dt max), minimum rate of pressure change in the ventricle (-dP/dt min) and the slope of the end diastolic pressure volume relationship (EDPVR).

Histological Analysis of Myocardial Collagen Content

Hearts were fixed in 10% formalin for histological analysis using picosirius red as previously described.⁵ Images were captured with brightfield microscopy using the Zeiss Imager D1, connected to a Zeiss AxioCam MRc5 colour camera and using AxioVision 40 version 4.7.1.0 acquisition software (Zeiss, Germany) with 10 images per section, from 2 sections per heart. Image analysis was performed using Image Pro Plus (V4.5.1, Media Cybernetics, MD, USA) in a 'blinded' manner. Briefly, images were converted to grey scale (255 pixel range), a pixel intensity histogram was assessed to determine the non-biased threshold point of collagen staining at 10% above the inflexion point in the histogram distribution. A binary map of collagen deposition was generated, from which collagen density was calculated and expressed relative to the total number of pixels in the area of interest. For each section, ten images per section positioned reproducibly at septal and ventricular free wall locations were analysed. In some images discrete areas of focal fibrosis were apparent. For all images a value of total fibrosis (expressed % area) was determined and the mean value for all image fields calculated. For those images where discrete fibrotic foci were apparent, an additional determination of mean 'interstitial fibrosis' was made excluding these areas.

Cardiomyocyte Structural Analysis by Tissue Section Confocal Microscopy

For ultrastructural analysis to examine cardiomyocyte sarcomeric integrity, high resolution confocal microscopy was performed using fixed tissues labelled with the fluorescent marker wheat germ agglutinin (WGA, Alexa-594) to delineate cardiomyocyte T-tubule geometry as previously described.^{6,7} Fluorescent images of labelled tissue sections were recorded with a Zeiss LSM410 confocal microscope using a Zeiss 63x NA 1.25 oil-immersion objective. Frequency analysis was used to assess the integrity of sarcolemmal T-tubular structure and the height of the peak at the sarcomere frequency of t-tubule labeling was used as one metric for integrity. The t-tubule images were converted to frequency space using the fast Fourier transform in the programming language IDL (Exelis). The height of the peak in the power spectrum corresponding to the sarcomere spacing (at $\sim 0.5 \mu\text{m}^{-1}$) was then estimated by fitting a Gaussian ('T power').

Cell Isolation and Cardiomyocyte Morphology

Electromechanical performance of fura-2 loaded isolated cardiomyocytes obtained from HHR and NHR hearts at age ~ 30 weeks was evaluated (HHR 33.6 ± 6.7 vs NHR 30.7 ± 6.4 weeks), a timepoint selected as a disease progression stage immediately prior to emergence of premature mortality in HHR. NHR and HHR animals were weighed and then killed by decapitation under deep isoflurane anaesthesia. Hearts were blotted and wet heart weight measured. Single ventricular myocytes were isolated enzymatically using methods previously described.^{5,8} Briefly, hearts were removed and perfused retrogradely on a Langendorff apparatus with Ca^{2+} -free bicarbonate-buffered physiological saline solution, maintained at 37°C , with the following composition (mM): NaCl, 118; KCl, 4.8; KH_2PO_4 , 1.2; MgSO_4 , 1.2; NaHCO_3 , 25, glucose, 11. Following 20 minutes of 0.45 mg/ml collagenase (Worthington; Type II) perfusion, hearts were removed from the perfusion apparatus, the left ventricle was isolated, placed in a conical flask and myocytes were dispersed by gentle agitation. Fractions containing viable cells were re-suspended at room temperature in 2-3 mls of HEPES-buffered physiological saline containing 1mM Ca^{2+} and were stored at room temperature. Cells were used within 8 hours. From each heart, 100 rod-shaped and regularly striated cardiomyocytes were selected randomly for length and width measurement at $\times 400$ magnification using a Nikon inverted light microscope and calibrated eye piece as previously described.^{5,8} Cell volume was

calculated from the product of cell length and cell width using the previously described relationship between these parameters,⁹ in which cell volume is calculated as $7.59 \times 10^{-3} \text{ pL}/\mu\text{m}^2 \times \text{cell area } (\mu\text{m}^2)$.

Whole-Cell Patch Clamp

I-Ca and I-NCX from NHR and HHR were measured in whole cell voltage clamp, using an Axopatch 200B patch-clamp amplifier (Axon Instruments, Foster City, CA) coupled to an A-D amplifier (Digidata 1200B, Axon Instruments) with 1-3 M Ω pipette resistances (glass type TW150F-3, World Precision Instruments, Sarasota, FL) as previously described.¹⁰ Prior to I-Ca and I-NCX measurements, membrane capacitance (C_m) was calculated from 5 mV hyperpolarizing and depolarizing steps applied from holding potential of -90 mV.

For I-Ca measurements, the pipette contained (in mM): CsCl 100, TEA-Cl 20, MgATP 5, Li-GTP 0.2, EGTA 10, HEPES 10, and pH 7.4 adjusted with CsOH at room temperature (22-25°C). Cells were superfused with normal Tyrode's solution containing (mM): NaCl 140, KCl 6, D-glucose 10, HEPES 5, MgCl₂ 1, CaCl₂ 1, and pH 7.4 adjusted with NaOH at room temperature. Once a successful 'break in' was obtained, the perfusion medium was switched to the modified normal Tyrode's solution containing (mM): TEA-Cl 140, CsCl 6, to replace NaCl, KCl respectively and pH 7.4 adjusted with TEA-OH. Voltage step protocols with three holding potentials (HP) were applied to identify the calcium currents available at different potentials: -115 mV (all currents), -90 mV (substantially excluding I-Ca_(TTX)) and -50 mV substantially excluding both I-Ca_(T) and I-Ca_(TTX). At each HP, test pulses were 400 ms depolarization and were made at test voltages ranging up to +60 mV, with steps of +10 mV increments (the interval between pulses was 2 s).

For I-NCX measurements, the solutions were adapted from Pogwizd *et al.* 1999.¹¹ The pipettes contained CsCl 45, Cs methanesulfonic acid 55, ATP-tris 10, GTP-tris 0.3, MgCl₂ 10.8, NaCl 14, CaCl₂ 2.21 (100 nmol/L free Ca), 1,2-bis (2 amino phenoxy) ethane-N,N,N',N'-tetra acetic acid (BAPTA) 5, Di-Br-1,2-bis (2 amino phenoxy) ethane-N,N,N',N'-tetra acetic acid (Di-Br BAPTA) 5, HEPES 20. To isolate I-NCX the normal Tyrode's solution was modified (CsCl 6 to replace KCl, CaCl₂ 2, BDM 30 and strophanthidin 10 $\mu\text{mol/L}$ to block Na/K-ATPase pump). To measure the I-NCX a combined voltage step and ramp protocol was applied.^{11,12} From an initial holding potential (HP) of -90 mV, the cell was depolarized to -45 mV (400 ms) to activate and inactivate Na current. Then a step from -45 mV to 0 mV (200 ms) was used to activate and inactivate I-Ca. Finally, the voltage was stepped to +80 mV (200 ms) and ramped down to -140 mV (1000 ms) to assess I-NCX. The protocol was repeated in the presence of 5 mM NiCl₂ to obtain Ni-sensitive I-Ca and I-NCX. To isolate I-NCX, the current traces were subtracted and the residual current measured during the +80 mV to -140 mV ramp was identified as I-NCX. Current analysis and curve fitting procedures were performed using Clampfit in pClamp8. For calculation of current density, currents were normalized by C_m. Current analysis and curve fitting procedures were performed using Clampfit in pClamp8. For calculation of current density, currents were normalized by C_m.

Cardiomyocyte intracellular Ca²⁺ and Contractility Measurements

Intracellular Ca²⁺ and cell length were measured simultaneously by microfluorimetry and edge detection (Ionoptix MA, USA) as previously described.¹³ Cells were loaded for 20 minutes with 2.5 μM fura-2/AM (Molecular Probes, Eugene, Or, USA) at room temperature. They were placed in a chamber mounted on the stage of an Olympus IX51 inverted fluorescence microscope and superfused with 1.5 mM Ca²⁺ HEPES solution, 37°C at a rate of 2ml/min and stimulated to contract at 3Hz. Excitation light at 360nm and 380nm was provided by a 75-watt xenon lamp and filter wheel. Emitted fluorescence (510 nm) was recorded by a photomultiplier tube, with the output current converted to voltage and digitized for subsequent analysis using the interpolated numerator method. Background correction was undertaken at the completion of each cell recording and incorporated into analysis protocol. The following calcium parameters were measured: diastolic Ca²⁺, systolic Ca²⁺, amplitude of the Ca²⁺ transient and time constant of decay of the Ca²⁺ transient (τ). Phase-loop plots of single cardiomyocyte contraction cycles through shortening and lengthening were

constructed to provide an indication of shift in cardiomyocyte Ca^{2+} sensitivity as previously described.¹³ In a pilot experiment sarcoplasmic reticulum Ca^{2+} load level in myocytes immediately following steady state contraction was determined by rapid and brief exposure of myocytes to 10mM caffeine. The peak of the Ca^{2+} contracture transient generated through store discharge via opened SR Ca^{2+} release channels was measured.

Cell length was measured using an edge detection system under basal conditions. For each contraction cycle, a range of normalized contractile parameters was automatically computed and averaged (% shortening (%S), time to peak shortening (Tm), maximum rate of shortening (mrs), maximum rate of lengthening (mrl) and time to cycle completion (Tf)). Cardiomyocyte performance was evaluated: (i) under basal paced conditions (37°C, 3Hz, 1.5mM Ca^{2+}), (ii) during a rest interval (37°C, 1.5mM Ca^{2+} 3Hz for 5 mins, stimulator off 30 secs), and (iii) with different inotropic challenges (4 mM Ca^{2+} , isoproterenol 10^{-8} M). All data were analyzed off-line using IonWizard (IonOptix, Milton, MA, USA).

Immunoblotting

Hearts were isolated and the blood flushed from the coronary vasculature with cold Krebs-Henseleit bicarbonate buffer (4°C). Ventricles were rapidly removed and snap frozen in liquid nitrogen. Ventricles were homogenized in 100mmol/L Tris-HCl, pH 7.0, phosphatase inhibitors NaF and Na_3VO_4 (at 5mmol/L and 0.5mmol/L respectively), and chelators EGTA and EDTA at 5mmol/L each (10mL buffer/g tissue) using an Ultra-Turrax tissue grinder (Crown Scientific, NSW, Australia). Non-fractionated homogenates were reconstituted in sodium dodecylsulphate (SDS) sample buffer. Samples were normalized for protein content.

SDS-polyacrylamide gel electrophoresis (SDS-PAGE) was performed, as previously described,¹⁴ using the Invitrogen XCell system (Invitrogen, VIC, Australia) using non-fractionated homogenate samples. After electrophoresis, proteins were transferred onto polyvinyl difluoride (PVDF) membranes using the XCell II blotter (Invitrogen, VIC, Australia). PVDF membranes were incubated in primary antibodies overnight at 4°C. Membranes were subsequently probed with the appropriate secondary antibody for 1 hour at room temperature and incubated in enhanced chemiluminescent reagent (Amersham ECL Plus, GE Healthcare) for 5 minutes. Protein bands were visualized with a Bio-Rad Chemi-XRS Imaging device, and band intensity was quantified using Quantity One imaging software (Bio-Rad). Representative Coomassie stained membranes (Fig S1B), confirmed equal loading of protein across all lanes in multiple gels used for each protein evaluation. In addition, dual calibrator control samples were included for all gels for every protein evaluated. Primary antibodies used in this study are tabulated (Fig S1A). For titin detection, protein bands and total phospho-protein levels were visualized using protein gel stains (Table S3).

Statistical Analyses

In general (unless otherwise stated) data are presented as mean \pm SEM. Sample sizes were estimated based on previous findings reported using similar techniques when possible. Comparisons between two groups with normally distributed data were performed with Student's unpaired t-test. Data from experiments with two groups assessed at multiple points were evaluated by a one-way analysis of variance (ANOVA) with repeated measures. Two-way ANOVA was used for evaluation of data groups comprising 2 factors. Correlation analyses were performed to determine the Pearson Coefficient within each strain and significance values evaluated. Data are shown depicting linear regression plots for each strain (SPSS c21.0; Graph Pad Prism V6). Data analysis was performed in a blinded manner. Survival (Kaplan Meier) data were analyzed by Log-rank Mantel-Cox test. Differences were considered significant at $P < 0.05$ (SPSS v.21.0; Graph Pad Prism V6).

Table S1. Echocardiographic and hemodynamic (cardiac catheterization) analysis of 50 week and 30 week HHR and NHR hearts.

Parameter		50 weeks		30 weeks	
		NHR	HHR	NHR	HHR
Echocardiography					
IVSd	(mm)	1.71 ± 0.04	2.20 ± 0.13*	1.76 ± 0.02	2.21 ± 0.06*
LVPWd	(mm)	1.89 ± 0.05	2.47 ± 0.23*	1.83 ± 0.08	2.62 ± 0.13*
LVIDd	(mm)	8.39 ± 0.12	9.21 ± 0.48	7.76 ± 0.12	8.87 ± 0.54
LVIDs	(mm)	5.01 ± 0.26	6.43 ± 0.36*	4.50 ± 0.20	5.96 ± 0.43*
FS	(%)	39.89 ± 2.2	30.35 ± 2.8*	42.14 ± 2.1	33.67 ± 1.1*
EF	(%)	74.6 ± 1.3	64.0 ± 3.8*	81.8 ± 1.6	73.2 ± 1.3*
HR	(bpm)	308 ± 6	352 ± 8*	312 ± 10	347 ± 7*
E wave velocity	(mm/s)	712 ± 54	1184 ± 121*	690 ± 34	1103 ± 65*
A wave velocity	(mm/s)	392 ± 23	885 ± 136*	383 ± 22	770 ± 87*
E/A ratio	(ratio)	1.86 ± 0.1	1.46 ± 0.14	1.83 ± 0.12	1.56 ± 0.14
MV Dec T	(ms)	61.1 ± 2.9	35.5 ± 4.5*	49.0 ± 3.8	26.8 ± 3.5*
E' velocity	(mm/s)	43.4 ± 4.4	46.9 ± 10.6	44.5 ± 3.5	35.2 ± 5.2
E/E'	(ratio)	16.9 ± 0.7	32.5 ± 4.6*	16.3 ± 1.0	33.3 ± 2.4*
Hemodynamic					
LVEDP	(mmHg)	10.6 ± 2.0	8.8 ± 1.9	N/A	N/A
+ dP/dt	(mmHg/s)	6200 ± 528	7894 ± 478*	N/A	N/A
- dP/dt	(mmHg/s)	5048 ± 532	5751 ± 465	N/A	N/A

IVSd – normalized interventricular septum at diastole (BW adjusted), LVPWd – normalized left ventricular posterior wall at diastole (BW adjusted), LVIDd – left ventricular inner diameter at diastole, FS – fractional Shortening, EF – ejection fraction, HR – heart rate, MV DecT – mitral valve deceleration time, LVEDP – left ventricular end diastolic pressure, + dP/dt – maximal slope of the systolic pressure increment, - dP/dt – maximal slope of the diastolic pressure decrement. (*p<0.05, 2-way ANOVA HHR vs NHR strain effect, n = 6 -10 hearts/group)

Table S2. HHR & NHR Cardiac and cardiomyocyte morphology during progression to failure (30 weeks).

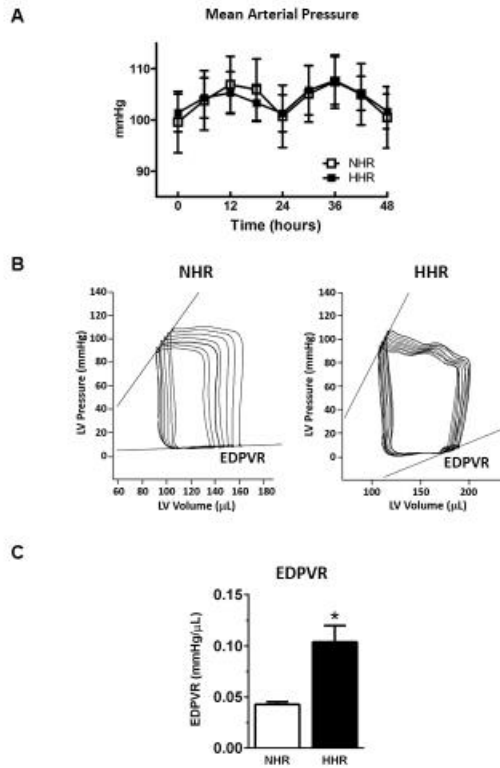
Parameter		NHR	HHR
CWI	(mg/g)	3.40±0.1 (39)	4.50±0.3* (34)
Myocyte Length	(mm)	132.5±0.99 (22)	163.1±2.3* (16)
Myocyte Width	(mm)	29.7±0.3 (22)	35.8±0.7* (16)
Myocyte Capacitance	(pF)	302.1±15.0 (18)	384.5±14.2* (16)
Myocyte Volume	(pL)	29.84±0.4 (22)	44.34±1.3* (16)

Significant elevation of cardiac weight and cardiac weight index in HHR, with increased cardiomyocyte size measured morphologically by dimensions, by computed volume and electrophysiologically (by capacitance). Calculated cardiomyocyte deficit of approx. 20% fewer cells/HHR heart (see Online Supplement regarding myocyte count calculation). (*p<0.05, Student's t-test, N hearts n parentheses, myocyte dimensions measured from mean n=50 cells per heart).

Table S3. Gel staining summary information.

Target Molecule	Name of Gel Stain	Manufacturer, catalogue #
Protein gel stain	SYPRO Ruby	Thermo Fisher Scientific (S12001)
Phosphoprotein gel stain	Pro-Q Diamond	Thermo Fisher Scientific (P33301)

Figure S1. Telemetry blood pressure (20-30 weeks) and LV hemodynamic measurements (50 weeks).

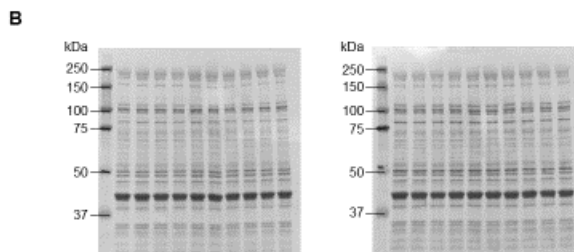


A. Equivalent (normotensive) diurnal mean arterial pressure (MAP) states in HHR and NHR. (mean \pm SD, n=6 HHR and NHR, age 20-30 weeks). **B.** Representative Pressure-Volume loops in NHR and HHR. **C.** Mean End Diastolic Pressure-Volume Relationship (EDPVR) measurements in HHR and NHR. For Panels B & C graphs show mean \pm SEM, n=8-9 HHR and NHR, age 50 weeks.

Figure S2. Immunoblot primary antibody summary information & Coomassie stained membranes.

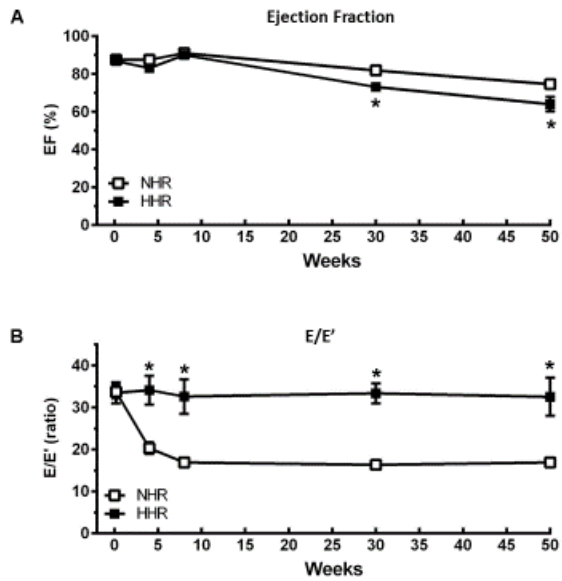
A

Peptide/protein target	Antibody	Manufacturer (catalogue #), and/or supplier	Species raised & clonal type
SERCA2a	SERCA2a	Badrilla (A010-20)	Rabbit polyclonal
Phospholamban	Phospholamban, clone A1	Upstate (05-205)	Mouse monoclonal
Phospholamban phospho Thr17	Phospholamban phospho Thr17	Badrilla (A010-13)	Rabbit polyclonal
Phospholamban phospho Ser16	Phospholamban phospho Ser16	Upstate (07-052)	Rabbit polyclonal
Ryanodine receptor	Ryanodine receptor [C3-33]	Abcam (ab2827)	Mouse monoclonal
Ryanodine receptor 2 phospho Ser2814	Ryanodine receptor 2 phospho Ser 2814	Badrilla A010-31	Rabbit Polyclonal
Ryanodine receptor 2 phospho Ser2808	Ryanodine receptor 2 phospho Ser2808	Upstate (07-052)	Rabbit polyclonal
CaMKIId	CaMKIId	Prof. DM Bers (UC Davis, USA)	Rabbit polyclonal
CaMKII phospho Thr287	CaMKII phospho T286	Abcam (Ab32678)	Rabbit polyclonal
Na ⁺ /Ca ²⁺ exchanger	Na ⁺ /Ca ²⁺ exchanger NCX1	Swant (π11-13)	Rabbit Polyclonal



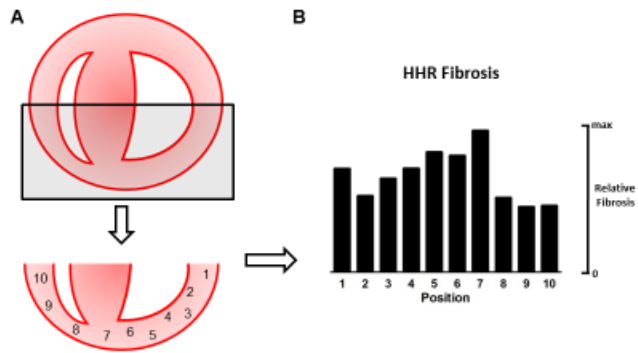
A. Immunoblot primary antibody summary information for HHR and NHR. **B.** Representative Coomassie stained membranes for HHR & NHR confirming equal loading of protein across all lanes.

Figure S3. Longitudinal systolic & diastolic NHR & HHR functional measurements.



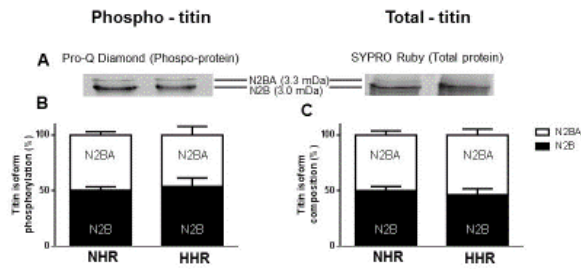
A. Mean changes in ejection fraction over 50 wks for HHR and NHR. **B.** Mean values for diastolic function ratio E/E' over 50 wks in HHR and NHR. (n=6-14 HHR and NHR, mean \pm SEM)

Figure S4. Locational fibrotic mapping of HHR cardiac transverse sections (age 50 weeks).



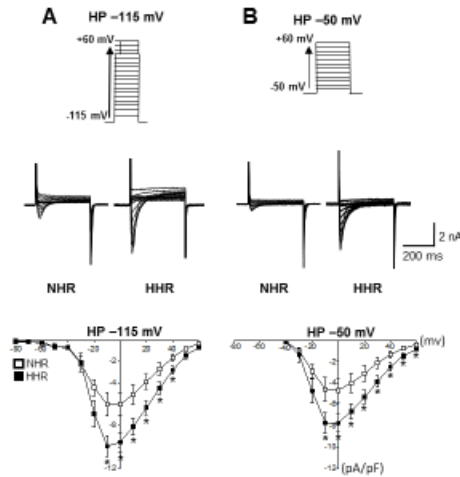
A. Schematic of transverse cardiac section indicating location of 10 image fields utilized for picrosirius analysis for all hearts. **B.** Mean relative fibrosis values from each of the ten locations, indicating more pronounced fibrosis at locations at/near position 7 and at position 1. (10 images per section, 2 sections per heart, N=5 hearts/group).

Figure S5. Titin-isoform composition and titin phosphorylation are unchanged in HHR (age 50 weeks).



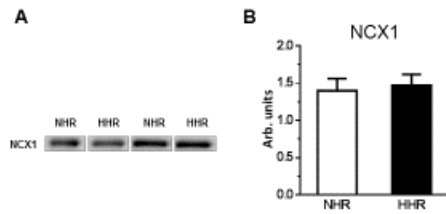
A. Representative immunoblot analyses of titin protein expression and phosphorylation levels from HHR and NHR left ventricular tissues. **B.** Titin isoform composition is not different between HHR and NHR. **C.** Total titin protein expression levels are not different between HHR and NHR (N=5 hearts/group).

Figure S6. Enhanced sarcolemmal Ca²⁺ current density in HHR vs NHR.



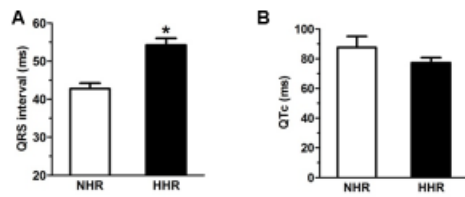
Voltage clamp protocol schematics, representative I-Ca current traces and mean normalized current-voltage plots obtained for voltage step protocols from two holding potentials (HP): **A.** HP-115mV; **B.** HP-50mV. Mean current densities (pA/pF) were significantly higher in the HHR at all holding potentials. (* $p < 0.05$, 1-way ANOVA with repeated measures, $n = 12-18$ cells/group). Graphs show mean \pm SEM, age 20-30 weeks (pre-failure).

Figure S7. NCX1 protein expression is unchanged in HHR (age 20-30 weeks).



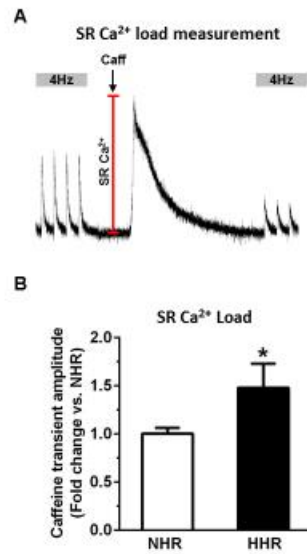
A. Representative immunoblot analyses of NCX1 protein expression from HHR and NHR left ventricular tissues. **B.** NCX1 protein expression is not different between HHR and NHR. (* $p < 0.05$, Student's t-test. $N = 10$ hearts/group). Graphs show mean \pm SEM.

Figure S8. NHR & HHR ECG parameters (age 50 weeks).



A. Mean QRS interval significantly extended in HHR. **B.** Mean QTc interval not different in HHR. (* $p < 0.05$, Student's t-test. $N = 8-12$ sample periods/heart, duration 10 sec). Graphs show mean \pm SEM.

Figure S9. Increased cardiomyocyte SR Ca²⁺ load in HHR.



A. SR load measurement protocol using caffeine (10mM) induced Ca²⁺ release preceded by 4Hz steady state stimulation. **B.** Caffeine transient amplitude expressed as mean fold change. (* $p < 0.05$, Student's t-test, $n = 10-20$ cells, for $N = 2-3$ hearts, $\text{mean} \pm \text{SEM}$).

Supplemental References:

1. Harrap SB, Danes VR, Ellis JA, Griffiths CD, Jones EF, Delbridge LM. The hypertrophic heart rat: A new normotensive model of genetic cardiac and cardiomyocyte hypertrophy. *Physiol Genomics*. 2002;9:43-48.
2. Innes BA, McLaughlin MG, Kapuscinski MK, Jacob HJ, Harrap SB: Independent genetic susceptibility to cardiac hypertrophy in inherited hypertension. *Hypertension* 1998;31:741-746.
3. Prestes PR, Marques FZ, Lopez-Campos G, Booth SA, McGlynn M, Lewandowski P, Delbridge LM, Harrap SB, Charchar FJ Tripartite motif-containing 55 identified as functional candidate for spontaneous cardiac hypertrophy in the rat locus cardiac mass 22. *J Hypertens*. 2016;34:950-8.
4. Zhang Y, Elsik M, Edgley AJ, Cox AJ, Kompa AR, Wang B, Tan CY, Khong FL, Stapleton DI, Zammit S, Williams SJ, Gilbert RE, Krum H, Kelly DJ. A new anti-fibrotic drug attenuates cardiac remodeling and systolic dysfunction following experimental myocardial infarction. *Int J Cardiol*. 201;168:1174-85.
5. Mellor KM, Bell JR, Young MJ, Ritchie RH, Delbridge LM. Myocardial autophagy activation and suppressed survival signaling is associated with insulin resistance in fructose-fed mice. *J Mol Cell Cardiol*. 2011;50:1035-1043.
6. Crossman DJ, Ruygrok PN, Soeller C, Cannell MB. Changes in the organization of excitation-contraction coupling structures in failing human heart. *PLoS One*. 2011;6:e17901.
7. Song LS, Sobie EA, McCulle S, Lederer WJ, Balke CW, Cheng H. Orphaned ryanodine receptors in the failing heart. *Proc Natl Acad Sci U S A*. 2006;103:4305-4310.
8. Domenighetti AA, Danes VR, Curl CL, Favalaro JM, Proietto J, Delbridge LM. Targeted glut-4 deficiency in the heart induces cardiomyocyte hypertrophy and impaired contractility linked with Ca²⁺ and proton flux dysregulation. *J Mol Cell Cardiol*. 2010;48:663-672.
9. Satoh H, Delbridge LM, Blatter LA, Bers DM. Surface:Volume relationship in cardiac myocytes studied with confocal microscopy and membrane capacitance measurements: Species-dependence and developmental effects. *Biophys J*. 1996;70:1494-1504.
10. Delbridge LM, Satoh H, Yuan W, Bassani JW, Qi M, Ginsburg KS, Samarel AM, Bers DM. Cardiac myocyte volume, Ca²⁺ fluxes, and sarcoplasmic reticulum loading in pressure-overload hypertrophy. *Am J Physiol*. 1997;272:H2425-2435.
11. Pogwizd SM, Qi M, Yuan W, Samarel AM, Bers DM. Upregulation of Na⁺/Ca²⁺ exchanger expression and function in an arrhythmogenic rabbit model of heart failure. *Circ Res*. 1999;85:1009-1019.
12. Hobai IA, Bates JA, Howarth FC, Levi AJ. Inhibition by external Cd²⁺ of Na/Ca exchange and l-type Ca channel in rabbit ventricular myocytes. *Am J Physiol*. 1997;272:H2164-2172.
13. Mellor KM, Wendt IR, Ritchie RH, Delbridge LMD. Fructose diet treatment in mice induces fundamental disturbance of cardiomyocyte Ca²⁺ handling and myofilament responsiveness *Am. J. Physiol. Heart Circ. Physiol*. 2012; 302:H964-972.

14. Bell JR, Porrello ER, Huggins CE, Harrap SB, Delbridge LM. The intrinsic resistance of female hearts to an ischemic insult is abrogated in primary cardiac hypertrophy. *Am J Physiol Heart Circ Physiol.* 2008;294:H1514-1522.